Rapid calculation of partition functions and free energies of fluids

Hainam Do, Jonathan D. Hirst, and Richard J. Wheatley

Citation: J. Chem. Phys. **135**, 174105 (2011); doi: 10.1063/1.3656296
View online: http://dx.doi.org/10.1063/1.3656296
View Table of Contents: http://jcp.aip.org/resource/1/JCPSA6/v135/i17
Published by the American Institute of Physics.

Rapid calculation of partition functions and free energies of fluids

Hainam Do, Jonathan D. Hirst,[a] and Richard J. Wheatley
School of Chemistry, University of Nottingham, University Park, Nottingham NG7 2RD, United Kingdom

(Received 2 June 2011; accepted 7 October 2011; published online 2 November 2011)

The partition function (Q) is a central quantity in statistical mechanics. All the thermodynamic properties can be derived from it. Here we show how the partition function of fluids can be calculated directly from simulations; this allows us to obtain the Helmholtz free energy (F) via $F = -k_BT \ln Q$. In our approach, we divide the density of states, assigning half of the configurations found in a simulation to a high-energy partition and half to a low-energy partition. By recursively dividing the low-energy partition into halves, we map out the complete density of states for a continuous system. The result allows free energy to be calculated directly as a function of temperature. We illustrate our method in the context of the free energy of water. © *2011 American Institute of Physics*. [doi:10.1063/1.3656296]

I. INTRODUCTION

Free energy provides the impetus for change in the natural world, whether in the formation of protein molecules or weather patterns, the destruction of cancer cells or the ozone layer. The estimation of free energies using computer simulation has been an active field for many decades, as it not only provides mechanistic insight at the atomic level, but also facilitates the study of systems not accessible experimentally.[1–11] Knowing the free energy allows one to predict many physical and chemical phenomena. Methods such as reversible thermodynamic integration[4] and free energy perturbation[5,12] provide the difference in the free energy between two states, but can be prohibitively expensive in terms of computing effort when applied to systems with large and complex changes, for example, calculations of solvation free energies of large solutes or calculations of the free energy of complex conformational changes.

Over the last three decades, several methods have been developed to calculate the density of states, Ω, from which the partition function, and hence, free energy can be obtained. Histogram reweighting,[13,14] transition matrix,[15] multicanonical,[3,16] and Wang-Landau[9] (W-L) sampling formalisms are examples of such methods. The drawback of these methods is that the density of states is determined through an iterative scheme. They rely on a histogram of energies to check the rate of convergence of a simulation, and can be inefficient when applied to systems with continuous energy levels. In addition, continuous systems require nontrivial extension of the original methods, which were designed for systems with discrete energy levels. A prerequisite is the requirement to discretize the entire infinite energy range. As yet, a systematic way of doing so has not been proposed. Therefore, one often has to choose a finite range of energy (either via trial-and-error or calculation) over which to determine the density of states.[17–20] This allows ensemble average properties to be calculated, but cannot give an accurate measurement of the free energy. Thus, free energy calculations still remain a big challenge in molecular simulation.

In this paper, we present a Monte Carlo technique that can systematically discretize a system comprising continuous energy levels and at the same time provide a direct calculation of the density of states. We demonstrate our method in the context of the free energy and vapor-liquid equilibrium of a molecular fluid (water), as it is difficult to obtain these data accurately, especially in the two-phase region. The calculated free energies from our method are compared with those calculated using the W-L sampling scheme. The W-L sampling is performed on the discretized energy subdivisions that are created by our method. The simulated vapor-liquid equilibrium properties are compared with those obtained from Gibbs ensemble[21] Monte Carlo simulations.

II. BACKGROUND

To compute the partition function and the free energy for interacting systems such as fluids, we have to integrate over all particle positions ($\mathbf{r}^N$) and velocities ($\mathbf{v}^N$) in the system. As the integration over particle velocities can be solved exactly, the partition function, in the canonical ensemble $Q(N, V, T)$, is

$$Q(N, V, T) = \frac{1}{N!\Lambda^{3N}} \int \exp[-\beta E(\mathbf{r}^N)] d\mathbf{r}^N, \qquad (1)$$

where N is the number of particles in the system. The factor $1/N!$ comes from the fact that particles are indistinguishable, Λ is the thermal de Broglie wavelength, E is configurational energy, β is $1/k_BT$, k_B is the Boltzmann constant, and T is the temperature of the system. For large systems with strong interactions between particles, the configurational space is enormously large and it is not possible to evaluate the integral in Eq. (1).

To introduce our algorithm, we write Eq. (1) in reduced coordinates ($\mathbf{s} = \mathbf{r}/L$) as

$$Q(N, V, T) = \frac{V^N}{N!\Lambda^{3N}} \int_0^1 \exp[-\beta E(\mathbf{s}^N)] d\mathbf{s}^N, \qquad (2)$$

[a]Electronic mail: jonathan.hirst@nottingham.ac.uk.

where L is the length of the cubic simulation box and V ($V = L^3$) is the volume of the box. The term $V^N/(N!\Lambda^{3N})$ in Eq. (2) is the partition function of an ideal gas, and can be calculated analytically. Thus, we seek to compute the excess part of the partition function (Q_{ex}), which is the Boltzmann factor averaged over all phase space:

$$Q_{ex} = \int_0^1 \exp[-\beta E(\mathbf{s}^N)]\mathrm{d}\mathbf{s}^N. \tag{3}$$

The probability of a configuration having an energy E is proportional to the density of states, $\Omega(E)$, where $\Omega(E) = \int_0^1 \delta(E - E(\mathbf{s}^N))\mathrm{d}\mathbf{s}^N$, and we can express Q_{ex} as

$$Q_{ex} = \frac{\int_{-\infty}^{\infty} \exp(-\beta E)\,\Omega(E)\,\mathrm{d}E}{\int_{-\infty}^{\infty} \Omega(\mathrm{E})\,\mathrm{d}E}, \tag{4}$$

where the integral is over all possible energies of the system. Equation (4) shows that if the density of states is known, the excess partition function can be calculated from it. In fact, $\Omega(E)$ contains even more information than Q and it may be possible to extract kinetic information from it, such as energy barrier crossing rates, which are important in the studies of systems with complex free energy landscapes, including proteins, polymers, and glasses. Moreover, as $\Omega(E)$ is independent of the temperature, the excess partition function can be obtained as a function of temperature from a single simulation. Equation (4) requires that we know both $\Omega(E)$ at high energy, which contributes most to the denominator, and $\Omega(E)$ at low energy, which contributes most to the numerator of Q_{ex}.

III. THE PARTITIONING METHOD

We now describe our method of discretizing the energy range and simultaneously obtaining the integrated normalized density of states for each energy subdivision. We need to subdivide the energy range more finely at low energy (Figure 1), as the Boltzmann factor changes rapidly there. At high energy, the subdivisions can be larger, as the only consideration is the density of states integrated over the subdivision. We divide the energy range recursively into subdivisions (indexed m), such that the integrated normalized density of states $\int_{E_m}^{E_{m-1}} \Omega(E)\,\mathrm{d}E / \int_{-\infty}^{\infty} \Omega(E)\,\mathrm{d}E$ equals $1/2^1$ for the first subdivision ($m = 1$, $E_1 \le E \le E_0$, $E_0 = \infty$), $1/2^2$ for the second subdivision ($m = 2$, $E_2 \le E \le E_1$), and so on down to $1/2^n$ for the two lowest energy subdivisions ($m = n$, $E_n \le E \le E_{n-1}$ and $m = n + 1$, $-\infty \le E \le E_n$), where n is the number of energy boundaries. Energy boundary 1 (E_1) is found first by division of the entire energy range. Then energy boundary 2 (E_2) is found by division of the energy range from $-\infty$ to E_1, and so on, to the last energy boundary n (E_n), which is found by division of the energy range from $-\infty$ to E_{n-1}.

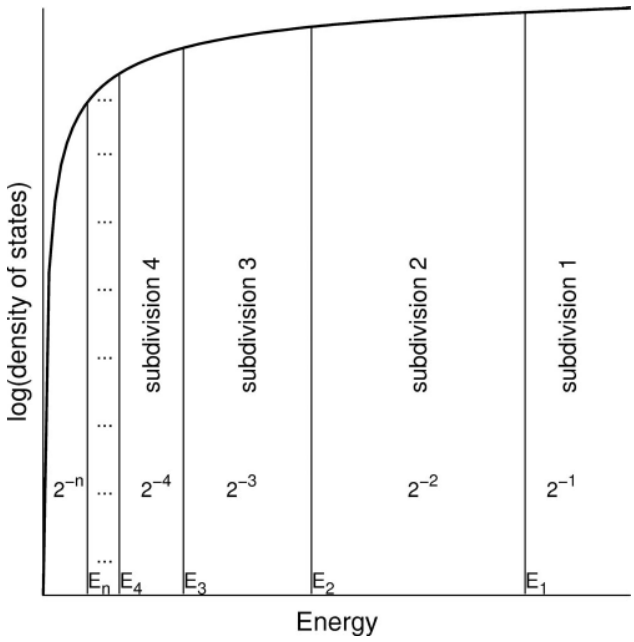

FIG. 1. Sketch (not to scale) explaining the partitioning of the density of states. n is the number of energy boundaries. Numbers denote the integrated normalized density of states over each subdivision.

For the mth division of the density of states (to produce energy boundary E_m), Monte Carlo sampling is performed. The first division of the energy, $m = 1$, does not employ any weighting function (random sampling). The subsequent ones are performed with a weighting function $w(E) = 4^i$ (the choice of this weighting function will be explained later in Sec. IV), where i is the energy subdivision into which the configurational energy E falls ($1 \le i \le m$), such that $E_i \le E \le E_{i-1}$ ($E_0 = \infty$, $E_m = -\infty$). The maximum translational move is set to a quarter of the length of the simulation box at the start of the simulation. The acceptance rate of any move is 100% for the first division regardless of the size of the move because random sampling is employed. It then decreases as m increases. Once m becomes large enough for the acceptance rate to drop to 20%, the maximum displacement is automatically adjusted after each energy division to keep an acceptance rate of about 20% throughout the rest of the simulation. Table I shows an example of the relative number of configurations $H(E)$ expected to occur in each energy subdivision during the 5th

TABLE I. Example showing the relative number of configurations $H(E)$ expected to occur in the first five energy subdivisions, during the 5th division of the energy ($m = 5$). The weighting applied in each subdivision is $w(E)$.

Subdivision i	5	4	3	2	1
Energy range	$-\infty \to E_4$	$E_4 \to E_3$	$E_3 \to E_2$	$E_2 \to E_1$	$E_1 \to \infty$
$\int_{E_i}^{E_{i-1}} \Omega(E)\,\mathrm{d}E / \int_{-\infty}^{\infty} \Omega(E)\,\mathrm{d}E$	2^{-4}	2^{-4}	2^{-3}	2^{-2}	2^{-1}
$w(E) = 4^i$	4^5	4^4	4^3	4^2	4^1
$H(E) = w(E)\left(\int_{E_i}^{E_{i-1}} \Omega(E)\,\mathrm{d}E / \int_{-\infty}^{\infty} \Omega(E)\,\mathrm{d}E\right)$	64	16	8	4	2

division of the energy (to produce energy boundary E_5). The sum of the geometric series in subdivisions 1 to 4 (all apart from the lowest energy subdivision) is 30, and in general it is less than half of the value of $H(E)$ in the lowest energy subdivision (here 64). Thus, this weighting function (4^i) ensures that at least 2/3 of the configurations of the system are expected to be in the current lowest energy subdivision (subdivision 5 in this example). Once sufficient data are collected (30 000 configurations) in the lowest energy subdivision, the next energy boundary E_{m+1} is set equal to the median configurational energy found in the lowest energy subdivision $-\infty \leq E \leq E_m$.

IV. SIMULATION DETAILS

The choice of the number of configurations used to determine each energy boundary and the choice of weighting function will influence the efficiency and accuracy of the simulations. Fewer configurations and a steeper weight function give faster calculations. However, this must be balanced with the accuracy. We first consider the effect of the number of configurations used to determine each energy boundary for our system of interest (300 water molecules) in both the liquid and the two-phase regions (Figures 2 and 3). The potential used for the water molecules and the simulation conditions are given in Sec. V. Successive configurations differ by an attempted move of one random molecule. These figures show that in the early stage of the partitioning process (first few hundred partitions), as few as 3000 configurations could be used to determine each energy subdivision, but the standard deviations are large (Figures 2(a) and 3(a)). As the number of energy subdivisions grows, the simulations require more configurations to equilibrate. So, to avoid a systematic error, we have to employ at least 18 000 configurations for the liquid phase (Figure 2(b)) and at least 27 000 configurations for the two-phase region (Figure 3(b)). Overall, the excess partition function is most accurately calculated with at least 18 000 configurations for the liquid phase (Figure 2(c)) and at least 27 000 configurations for the two-phase region (Figure 3(c)). Thus, for a system of 300 water molecules, we find that 30 000 configurations are reasonable (based on the information given in Figures 2 and 3) for each division of the energy.

A biased weighting function is necessary in our algorithm to speed up the calculations. If no biased weighting function were used ($w(E) = 1$), which is done for the first division of the energy, then we would hardly ever visit the low-energy region. On the other hand, too steep a weighting function could reduce the flexibility of the system to explore the configurational space. Every energy subdivision can be visited an equal number of times by employing $w(E) = 2^i$ (apart from the lowest energy subdivision, which is visited twice as often). This still leads to inadequate sampling of the lowest energy subdivision when there are hundreds of subdivisions. Thus, a weighting function steeper than 2^i needs to be employed. For example, with $w(E) = 3^i$ or $w(E) = 4^i$, about 1/2 or 2/3 of the total configurations are expected to be in the lowest subdivision, respectively. The steeper the weighting function is, the more configurations are in the lowest energy subdivision. Figure 4 shows that the energy boundaries and excess

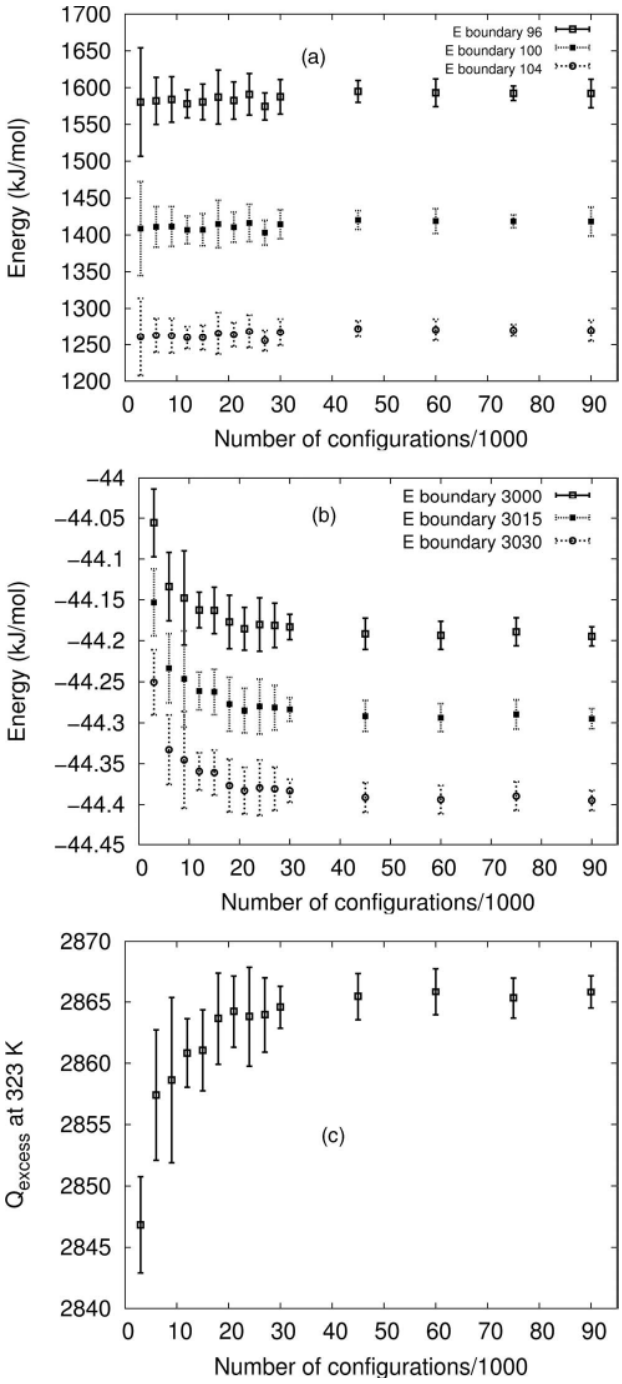

FIG. 2. Effect on the partitioning method of the number of configurations used to determine each energy boundary (liquid phase $\rho = 1000.0$ kg/m^3). (a) Errors in selecting the energy boundary in the high-energy region. (b) Errors in selecting the energy boundary in the low-energy region. (c) Errors in the excess partition function. The total number of energy boundaries required under these conditions is about 3800. The standard deviations are determined by performing a set of 15 different simulations.

partition function can be accurately calculated with a very steep weighting function (up to $w(E) = 32^i$) for 300 water molecules. However, the error bars are generally bigger for steeper weighting functions. To give the system the flexibility to explore the configurational space, we should employ a weighting function that is not too steep. A weighting function

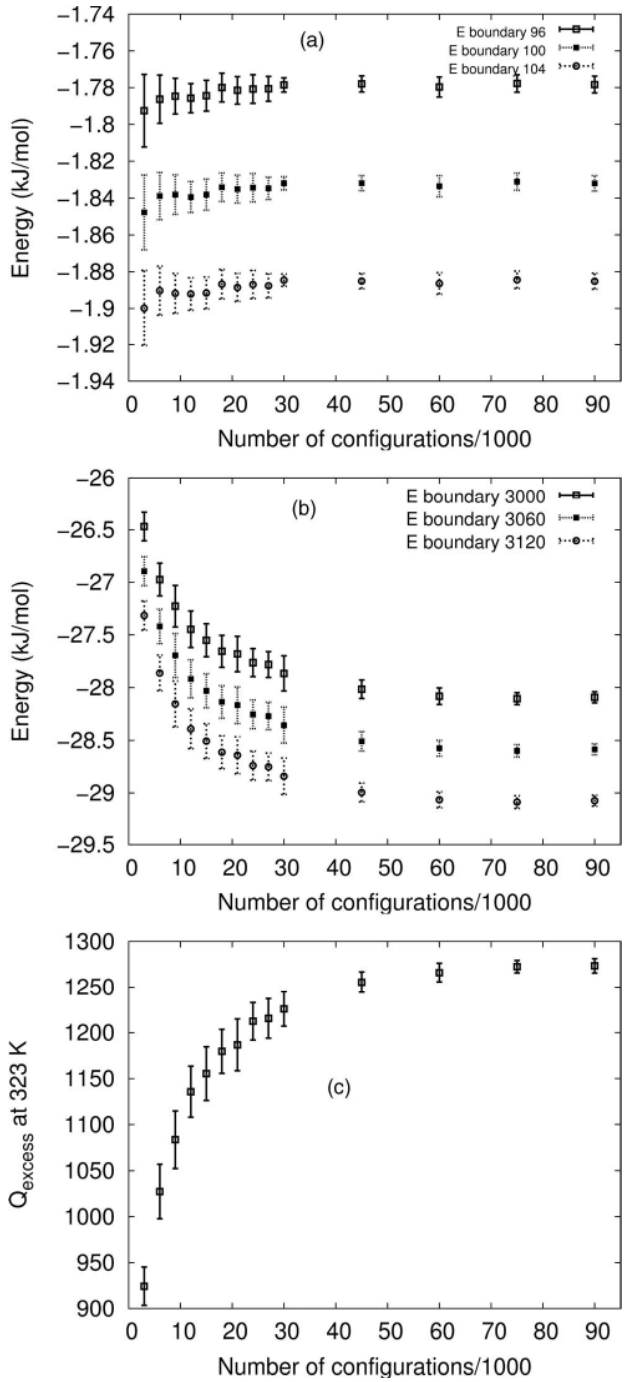

FIG. 3. Effect on the partitioning method of the number of configurations used to determine each energy boundary (two-phase region $\rho = 15.0\ \mathrm{kg/m^3}$). (a) Errors in selecting the energy boundary in the high-energy region. (b) Errors in selecting the energy boundary in the low-energy region. (c) Errors in the excess partition function. The total number of energy boundaries required under these conditions is about 5500. The standard deviations are determined by performing a set of 15 different simulations.

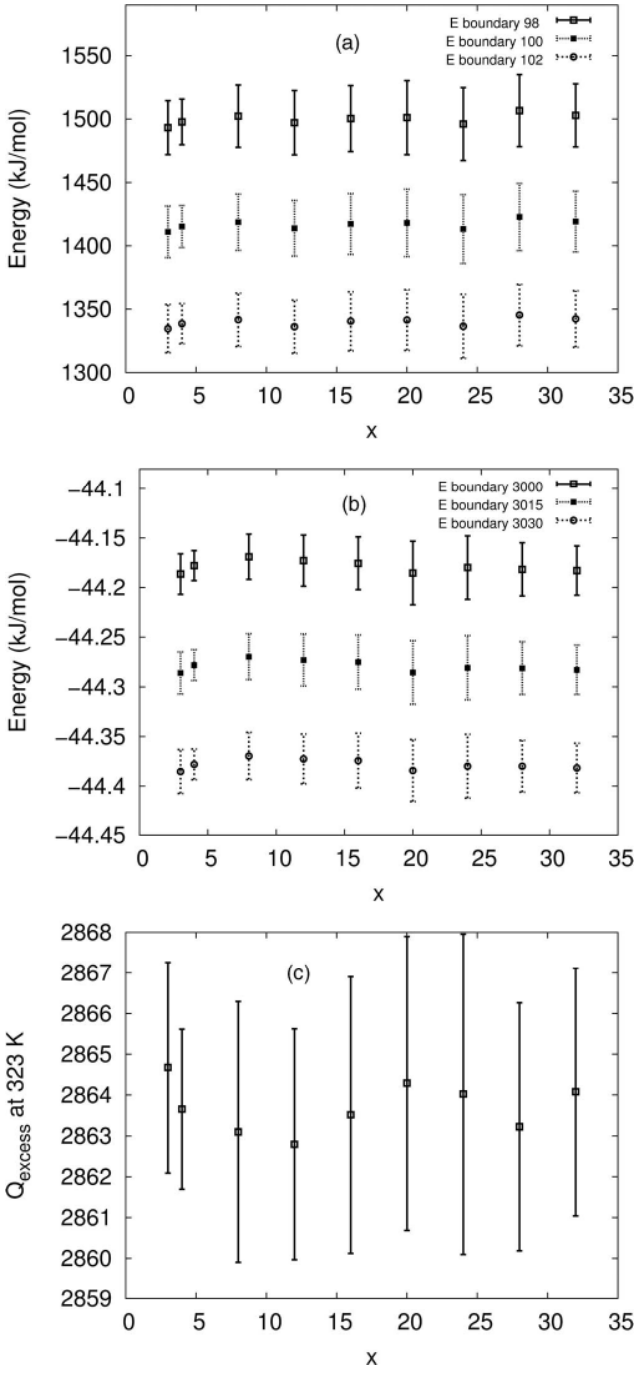

FIG. 4. Effect on the partitioning method of the choice of weighting function (liquid phase $\rho = 1000\ \mathrm{kg/m^3}$). (a) Errors in selecting the energy boundary in the high-energy region. (b) Errors in selecting the energy boundary in the low-energy region. (c) Errors in the excess partition function. $w(E) = x^i$, if energy E is in subdivision i. The total number of energy boundaries required under these conditions is about 3800. The standard deviations are determined by performing a set of 15 different simulations.

$w(E) = 4^i$ gives us good balance between the efficiency and accuracy of the simulations.

We note that $\Omega(E)$ strongly increases with energy (except at very high energy), $\exp(-\beta E)$ strongly decreases with energy, and the function $\Omega(E)\exp(-\beta E)$ is peaked around an average energy. We stop dividing the energy once we reach a point where $\Omega(E)\exp(-\beta E)$ is much smaller than $[\Omega(E)\exp(-\beta E)]_{\max}$. We find that $\Omega(E)\exp(-\beta E) = 10^{-9}[\Omega(E)\exp(-\beta E)]_{\max}$ is sufficient. This stopping criterion is temperature-dependent and we use the lowest temperature of interest, in order to cover all the important parts of the energy range. The excess partition function is

obtained from the normalized integrated density of states as

$$Q_{ex} = \frac{\sum_{m=1}^{m=n+1} \left(\int_m^{m-1} \Omega(E)\mathrm{d}E\right) \exp\left(-\beta \langle E\rangle_m\right)}{\sum_{m=1}^{m=n+1} \int_m^{m-1} \Omega(E)\mathrm{d}E} = \frac{\sum_{m=1}^{m=n+1} 2^{-m} \exp\left(-\beta \langle E\rangle_m\right)}{\sum_{m=1}^{m=n+1} 2^{-m}}, \quad (5)$$

where $\langle E\rangle_m = (E_n + E_{n-1})/2$. For the first ($m = 1$) subdivision (Figure 1), we set $\langle E\rangle_m = E_1$, and for the last ($m = n + 1$) subdivision we set $\langle E\rangle_m = E_n$ and replace 2^{-m} by 2^{-n}.

V. CASE STUDY FOR WATER

In this work, we calculate the partition function, free energy, and vapor-liquid equilibrium properties of water, as an example of a real molecular fluid of interest. The SPC-E model[22] for water is employed. The fluid is simulated in a cubic box with periodic boundary conditions. A spherical cut-off of half of the length of the simulation box is used to truncate the Lennard-Jones interactions. A long-range correction for the r^{-6} term (tail correction)[23] is used: $E_{\text{tail}} = -64\pi\rho\varepsilon\sigma^6/3V$, where ρ is the density of molecules in the simulation box. The r^{-12} term decays rapidly with distance, so a correction for this term is unnecessary. Ewald summation with the tinfoil boundary condition is used to calculate the electrostatic interactions.[24] For 300 water molecules at 298.15 K and a density of 1000 kg/m^3, the maximum value of $\log[\Omega(E)\exp(-\beta E)]$ is 3289.25, and occurs at an energy of −46.83 kJ/mol and energy boundary $n = 3432$ (Figure 5). The partitioning for this system stopped when $\log[\Omega(E)\exp(-\beta E)]$ reached 3268.24, at an energy of −49.21 kJ/mol and energy boundary $n = 3878$.

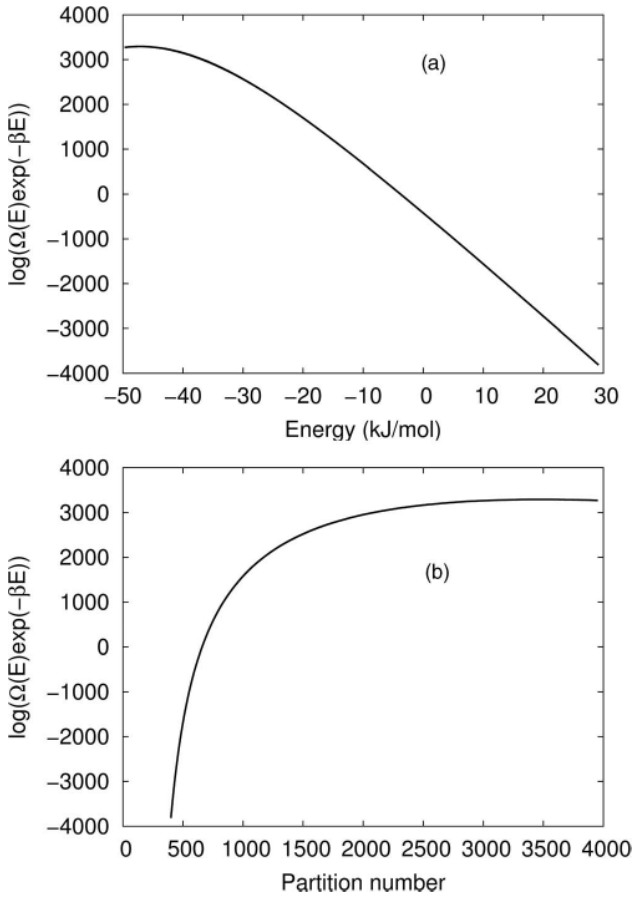

FIG. 5. $\log(\Omega(E)\exp(-\beta E))$ versus energy (a) and partition number (b) for 300 water molecules at $T = 298$ K and $\rho = 1000$ kg/m^3.

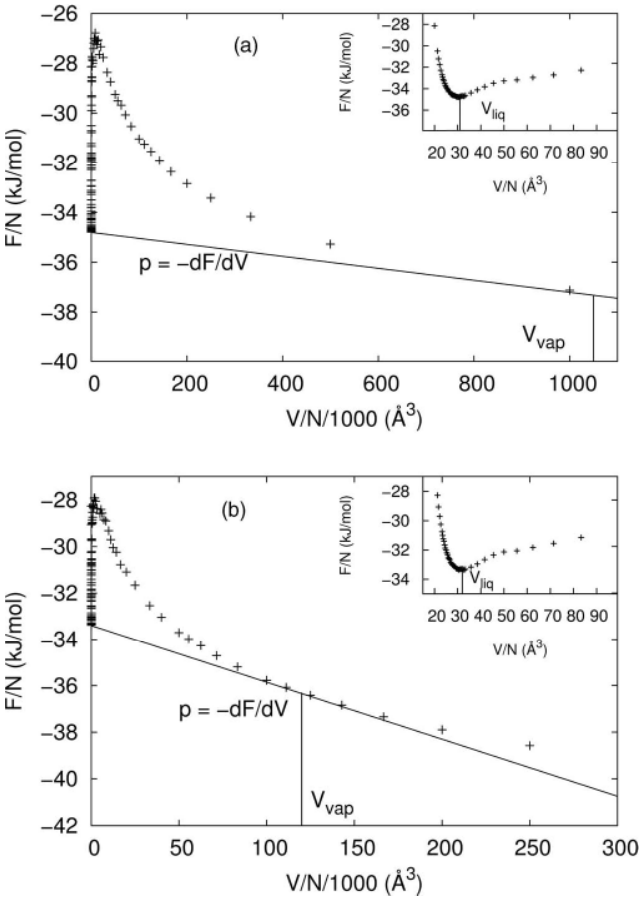

FIG. 6. Helmholtz free energy per particle versus volume per particle for 300 water molecules at (a) 323.15 K and (b) 373.15 K. Insets show a magnification of the local minima. The error bars are too small to show on the plot. The standard errors are determined by performing a set of 15 different simulations for each density. In most cases, the standard errors are between 0.2% and 0.3%.

After the partitioning process is complete, the entire energy range has been discretized into $n + 1$ energy subdivisions. The excess partition function is obtained using Eq. (5) and the excess free energy (F_{ex}) is obtained from $F_{\text{ex}} = -k_B T \ln Q_{\text{ex}}$. The density dependence of the ideal gas free energy is $F_{\text{id}} = -k_B T \ln\rho$, and the total density-dependent part of the free energy is $F_{\text{ex}} + F_{\text{id}}$. Figure 6 shows the free energy ($F_{\text{ex}} + F_{\text{id}}$) per particle versus volume per particle for 300 water molecules. The coexisting volumes are determined by constructing a double tangent. The coexisting pressure is the slope of this tangent line ($-\mathrm{d}F/\mathrm{d}V$). The latent heat of vaporization equals $(\langle E\rangle_{vap} - \langle E\rangle_{liq}) + p(V_{vap} - V_{liq})$, where

$$\langle E\rangle = \frac{\sum_{m=1}^{m=n+1} \langle E\rangle_m 2^{-m} \exp\left(-\beta \langle E\rangle_m\right)}{\sum_{m=1}^{m=n+1} 2^{-m} \exp\left(-\beta \langle E\rangle_m\right)}.$$

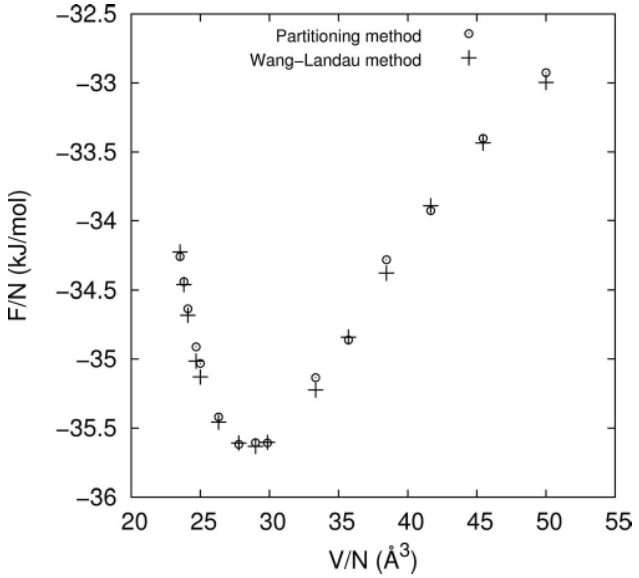

FIG. 7. A comparison between the Helmholtz free energy per particle calculated using our method (circles) and W-L method (pluses) for different densities at 323.15 K. The calculations were performed for systems of 64 water molecules. The error bars for our method are too small to show. Values from W-L simulations are recorded at the last convergence factor f ($f < 10^{-8}$).

Given the energy subdivisions created by our method, we can also perform a W-L sampling to estimate the integrated density of states of each energy subdivision. Note that performing a W-L sampling here is redundant, as the integrated density of states of each subdivision have already been determined during the energy partitioning process (2^{-m}). However, we perform W-L sampling here to compare the accuracy and efficiency of the two methods. At the start, a constant integrated density of states is assumed for all subdivisions. Every time a subdivision is visited, its integrated density of states is multiplied by a convergence factor f, where $f = \mathrm{e}(2.72)$ at the start. An energy histogram $H(E)$ of the energy subdivisions is accumulated during the course of the simulation. When $H(E)$ becomes sufficiently flat (the subdivision with minimum number of hits is within 80% of the mean number of hits per subdivision), f is reduced to $\sqrt{f}$ and $H(E)$ is reset to zero. The simulations stop when $f < 10^{-8}$. Figure 7 shows a comparison of the free energies calculated by our method and the W-L method for different densities in the liquid phase of water at 323.15 K. The results from our method agree very well with those obtained using W-L sampling. Since the W-L algorithm involves an iterative scheme, it is highly inefficient compared to our method. In the best case, the W-L method still requires over 100 times the number of configurations required by our method and this number can rise as high as a factor of about 1000 in some cases (Table II).

To validate our method further, we also show that the vapor-liquid equilibrium properties calculated using our

TABLE II. Number of configurations (N_{config}) required by our partitioning method, and that required by the W-L method (excluding the effort in discretizing the energy levels), at different densities in the liquid phase of water, for a system of 64 molecules.

Number density (Å^{-3})	$N_{config}^{partitioning}/10^6$	$N_{config}^{W-L}/10^6$
0.020	27.30	5600
0.022	28.11	11 850
0.024	27.57	8660
0.026	27.63	3920
0.028	29.19	23 900
0.030	28.86	14 370
0.036	29.43	7070
0.040	29.46	12 550

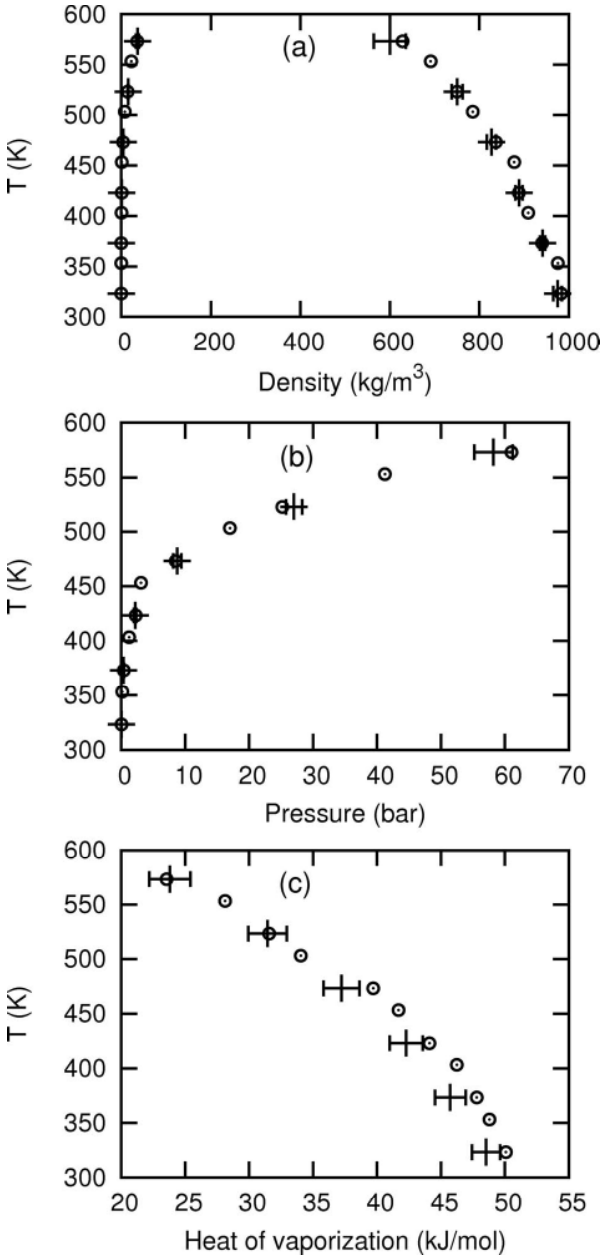

FIG. 8. Vapor-liquid coexistence densities (a), temperature-pressure equilibrium curve (b), and the latent heat of vaporization (c) of water (using the SPC-E model): our method (circles) and Gibbs ensemble simulations (pluses). Both methods employ 300 water molecules.

method agree well with those calculated by the Gibbs ensemble technique using in-house software (Figure 8). As the Gibbs ensemble technique is temperature-dependent, its efficiency depends on the number of state points that are required to be calculated. Our method, on the other hand, is temperature-independent and does not suffer from this shortcoming.

VI. CONCLUSION

The proposed method provides the density of states without iteration, and is much more efficient than the W-L approaches. Moreover, our method is more robust than the W-L method when dealing with continuous systems, as it accompanies a systematic scheme to discretize the continuous energy levels so that the important aspects of the configurational space are included. The excess partition function and free energy are obtained directly from the density of states. Our method simplifies the process of calculating free energies of continuous systems, and could have an impact in many applications, including the study of phase equilibria, solvation free energy, nucleation dynamics, protein folding, and DNA folding. The method can be easily extended to study systems with discrete energy levels, for which there are also a large number of applications, including spin glasses and lattice models of proteins and polymers.

ACKNOWLEDGMENTS

We thank the University of Nottingham High Performance Computing facility for providing computer resources and the Engineering and Physical Sciences Research Council (EPSRC) for funding (Grant No. EP/E06082X). H. Do is grateful to the EPSRC for a PhD Plus Fellowship.

[1] P. A. Bash, U. C. Singh, R. Langridge, and P. A. Kollman, Science **236**, 564 (1987).
[2] P. A. Bash, U. C. Singh, F. K. Brown, R. Langridge, and P. A. Kollman, Science **235**, 574(1987).
[3] B. Berg and T. Neuhaus, Phys. Lett. B **267**, 249 (1991).
[4] J. Hansen and L. Verlet, Phys. Rev. **184**, 151 (1969).
[5] D. Henderson and J. A. Barker, Phys. Rev. A **1**, 1266 (1970).
[6] D. Levesque and L. Verlet, Phys. Rev. **182**, 307 (1969).
[7] S. N. Rao, U. C. Singh, P. A. Bash, and P. A. Kollman, Nature **328**, 551 (1987).
[8] M. D. Tyka, R. B. Sessions, and A. R. Clarke, J. Phys. Chem. B **111**, 9571 (1987).
[9] F. G. Wang and D. P. Landau, Phys. Rev. Lett. **86**, 2050 (2001).
[10] R. P. White and H. Meirovitch, Proc. Natl. Acad. Sci. U.S.A. **101**, 9235 (2004).
[11] Q. Yan, T. S. Jain, and J. J. de Pablo, Phys. Rev. Lett. **92**, 235701 (2004).
[12] R. W. Zwanzig, J. Chem. Phys. **22**, 1420 (1954).
[13] A. M. Ferrenberg and R. H. Swendsen, Phys. Rev. Lett. **61**, 2635 (1988).
[14] A. M. Ferrenberg and R. H. Swendsen, Phys. Rev. Lett. **63**, 1195 (1989).
[15] J. S. Wang, T. K. Tay, and R. H. Swendsen, Phys. Rev. Lett. **82**, 476 (1999).
[16] C. J. Geyer and E. A. Thompson, J. Am. Stat. Assoc. **90**, 909 (1995).
[17] G. Ganzenmuller and P. J. Camp, J. Chem. Phys. **127**, 154504 (2007).
[18] M. S. Shell, P. G. Debenedetti, and A. Z. Panagiotopoulos, Phys. Rev. E **66**, 56703 (2002).
[19] M. S. Shell, P. G. Debenedetti, and A. Z. Panagiotopoulos, J. Chem. Phys. **119**, 9406 (2003).
[20] Q. Yan, R. Faller, and J. J. de Pablo, J. Chem. Phys. **116**, 8745 (2002).
[21] A. Z. Panagiotopoulos, Mol. Phys. **61**, 813 (1987).
[22] H. J. C. Berendsen, J. R. Grigera, and T. P. Straatsma, J. Phys. Chem. **91**, 6269 (1987).
[23] D. Frenkel and B. Smit, *Understanding Molecular Simulation: From Algorithms to Applications* (Academic, San Diego, 2002).
[24] M. P. Allen and D. J. Tildesley, *Computer Simulation of Liquids* (Clarendon, Oxford, 1987).